Journal of Applied Research and Technology

www.jart.icat.unam.mx

Journal of Applied Research and Technology 24 (2026) 409-422

Original

Analysis of the efficiency of the geothermal dryer and its effect on the kinetic mass transfer parameters

Sahylin Muñiz-Becerá[a*] • Héctor Miguel Aviña-Jiménez[a]
Brenda Cecilia Alcántar-Vázquez[a] • Rodrigo Alarcón[a]
Mariana Patricia Jácome-Paz[b].

[a]Instituto de Ingeniería, Universidad Nacional Autónoma de México, Ingeniería S/N, C.U., Coyoacán, 04510, Ciudad de México, CDMX.
[b]Instituto de Geofísica, Universidad Nacional Autónoma de México, Circuito de la Investigación Científica s/n, C.U., Coyoacán, 04150 CDMX

Received: 27 06 2024; Accepted: 27 04 2025
Available: 30 04 2026

Abstract: Geothermal energy is an efficient alternative for convective drying of food. This research aimed to determine the efficiency of a low-temperature geothermal dryer (LTGE) system in dehydrating high-moisture foods and its effects on the kinetic parameters and properties of the dehydrated foods. This study used a prototype laboratory-scale geothermal dehydrator built at the Geothermal Laboratory of the Engineering Institute of UNAM. The influence of the geothermal dehydrator operating parameters- average temperature (60, 65, 70 °C) and airflow velocity (2.5, 3.0, 3.3 m/s) on moisture content kinetics, drying rate, moisture-effective diffusion coefficient (D_{eff}), physicochemical properties, and drying efficiency was determined. The results indicated that mean temperature and airflow rate influenced the drying kinetics and properties of dried apples and mangoes. With increasing temperature and airflow velocity, the drying rate and effective diffusion coefficient increased. The drying curves were dominated by the period of decreasing rate, which is typical of the drying kinetics of biological materials under constant-temperature conditions. The increase in temperature and airflow velocity increased the effective diffusion coefficient and drying efficiency. The D_{eff} ranged from 0.43–8.59 x 10^{-9} m^2/s for the dried apple

*Corresponding author.
E-mail address: smunizb@iingen.unam.mx (Sahylin Muñiz Becerá).
Peer Review under the responsibility of Universidad Nacional Autónoma de México.

samples and from 5.54–8.92 x 10^{-9} m^2/s for the dehydrated mango samples. Moisture content curves showed moisture contents below 10% at drying times similar to those achieved with a conventional convective dryer, demonstrating that geothermal energy can be used for fruit dehydration, producing high-quality dehydrated products and enabling efficient drying processes.

Keywords: **geotermal drying; efficiency; kinetic parameters; food properties**

1. Introduction

In the food industry, energy consumption for food drying accounts for 10% of total energy demand (Li et al., 2019; Yahya et al., 2022). Using renewable energy for food drying, such as geothermal energy, is an alternative to reduce fossil fuel use and promote the transition to clean energy in this sector. Mexico has high geothermal energy potential, which has been used primarily for electric power generation. However, medium- and low-enthalpy geothermal energy can be used efficiently in industrial processes that require heat, such as drying agricultural products such as fruits, vegetables, and grains.

In terms of renewable energy, solar drying has been the most commonly used conventional method for dehydrating fruit. However, both open-air solar drying as in solar dryers have the disadvantage of variable temperature air, due to the daily and seasonal changes in solar intensity in the limited time that sunlight is available during the day making the solar drying process intermittent, causing impairments in the quality properties of the dehydrated product due to excessive drying times, which require several days of processing, especially in foods with high moisture content such as fruits. Recently, there has been growing interest in the direct use of geothermal heat for processes that require heat, such as food drying (Andritsos et al., 2003; Helvacı & Akkurt, 2014; Prasetyo et al., 2018; Sircar et al., 2021). The implementation of a geothermal dehydrator system for fruit preservation is attractive due to the advantages of geothermal energy for continuous processes such as drying: constant temperature due to geothermal fluid flow at a constant rate throughout the year, making it a continuous resource. The constant temperature and airflow speed during the geothermal drying process result in improved dried product quality and reduced drying time.

Some studies have addressed the design and evaluation of geothermal dryers (Helvacı & Akkurt, 2014; Prasetyo et al., 2018; Sircar et al., 2021). However, few reports in the literature explore the effects of different drying temperatures and airflow rates on the drying efficiency using geothermal energy, kinetic parameters, and changes in food properties during the process. Drying efficiency and kinetic parameters: moisture content, drying rate, and effective diffusivity coefficient play an important role in evaluating the design of the geothermal food dehydrator system and optimizing the geothermal drying process. The main objectives of this research are presented as follows: 1) To explore the effects of drying temperature and airflow rate on the drying efficiency of food using geothermal energy; 2) To analyze the influence of drying temperature and airflow rate on drying kinetics: moisture content, drying rate, mass transfer, and activation energy; 3) Determine the effect of geothermal drying parameters on the main properties of dehydrated food.

2.Materials and methods

2.1 Description of the geothermal dryer system.

The experimental study was conducted in a laboratory-scale geothermal food dehydrator (GFD) prototype. The working principle of the geothermal food dehydrator is shown in Figure 1. The low-enthalpy geothermal fluid was simulated by using a water heater (Rheem, model 89VP20). A hydraulic circuit was installed to circulate hot water, driven by a recirculation pump (Truper pressurized pump, 1/6 HP). The water leaves the storage tank and passes through the electric water heater (Rheem, model 89VP20) to gain the necessary thermal energy. The heater capacity is 9 kW, and the pump capacity is 15 L/m. Finally, the hot water enters the upper head of the finned tube heat exchanger (IC-SV-01) to avoid thermal shock, and the air enters at a medium temperature and ends at a high temperature, similar to a heating process (preheating). The ambient air is sucked in by the centrifugal fan and propelled around the finned tubes of the heat exchanger. As the temperature increases, the hot air flows by convection towards the drying chamber. The fan

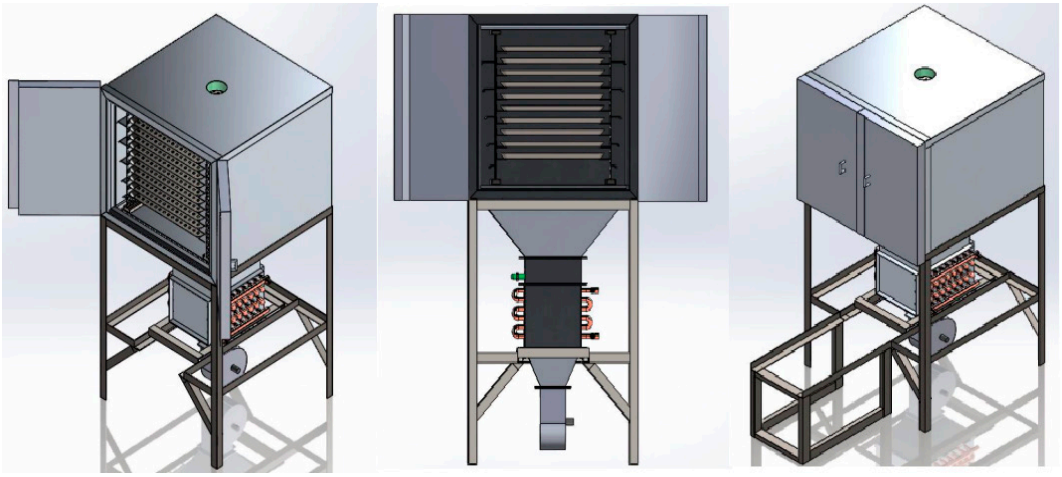

Figure 1. Schematic diagram of geothermal drying.

speed is adjusted up to 2 m/s by the inverter, with the air flowing from the air inlet through the drying chamber. In the drying chamber, hot air from convection evaporates moisture from the food and exits through a chimney. The drying chamber has a cabinet with two columns of racks that support the trays with the dehydrated food. The chamber was constructed from 19 mm aluminum sheets, measuring 0.7 m × 0.50 m × 0.550 m (length × width × height). During drying, hot air enters through the bottom of the chamber and is directed to the trays by the centrifugal fan, which is equipped with a filter to prevent food contamination. The schematic of the dryers used is shown in Figure 1.1, and the geothermal dryer laboratory prototype is shown in Figure 2.

Figure 2. Geothermal dryer system laboratory prototype.

2.2. Experimental procedures

Sample preparation

Apple (*var. Red Delicious*) and mango (*var. Paraiso*) were purchased at a local market. The criterion for fruit selection was firm to touch and with no visible physical damage. The same fruit lot was used in each experiment to minimize biological variability and changes in cellular structure. The fruits were washed and disinfected with a colloidal silver solution (0.05% w/w). Then, fruits were cut into longitudinal slices 5±0.15 mm thick using a stainless-steel slicer and placed on trays.

Geothermal drying process

To study the geothermal drying process, a frequency converter was installed on the fan motor. For each frequency value, an airflow speed and, therefore, a different temperature value were obtained inside the drying chamber. The experimental variants are presented in Table 1.

V_1—experimental variant for apple dried at 60 °C and airflow speed: 2.5 m/s; V_2—experimental variant for apple dried at 65 °C and airflow speed: 3 m/s; V_3—experimental variant for apple dried at 70 °C and airflow speed: 3.3 m/s; V_4—experimental variant for mango dried at 60 °C and airflow speed: 2.5 m/s; V_5—experimental variant for mango dried at 65 °C and airflow speed: 3 m/s; V_6—experimental variant for mango dried at 70 °C and airflow speed: 3.3 m/s.

Finally, the geothermal drying process for the fruits was carried out at average temperatures of 60, 65, and 70 °C and airflow speeds of 2.5, 3.0, and 3.3 m/s.

Table 1. Experimental variations regarding the geothermal drying of fruits, according to temperature in the dryer chamber and airflow velocity.

Products	Experimental Variants	Frequency (Hz)	Mean drying temperature (°C)	Mean airflow velocity (m/s)	Activity
Apple	V_1	20	60	2.5	Mass-transfer kinetic parameter determination: moisture content, drying rate, effective diffusivity, drying efficiency. Physical and chemical determination: moisture content in dry matter; color index and °Brix.
Apple	V_2	30	65	3	
Apple	V_3	40	70	3.3	
Mango	V_4	20	60	2.5	
Mango	V_5	30	65	3	
Mango	V_6	40	70	3.3	

Geothermal drying efficiency

Drying efficiency is a critical factor in the geothermal food-drying process. It measures how effectively the drying system removes moisture from the product and significantly affects the final dried product's quality and shelf life.

In the literature, drying efficiency is calculated in two ways: the first is by comparing the amount of moisture removed from the material with the amount of energy used in the drying process, it the initial and final material moisture content must be determined, as well as the energy consumption during the drying (Djaeni et al., 2019). Air humidity and temperature were measured by a T-RH sensor (HOBO, model MX2302). The recorded data were used to calculate drying efficiency during the geothermal drying process, and the following equations were used:

$$\eta = \frac{Q_{evap}}{Q_{ca}} \bullet 100(\%) \quad (1)$$

$$Q_{evap} = w_p(X_{w,o} - X_{w,f}) \cdot \lambda \quad (2)$$

$$Q_{ca} = C_{pa} \cdot m_a \cdot \Delta T \quad (3)$$

Where: η- Drying efficiency (%); Q_{evap}-total heat to evaporate water from product (kJ); Q_{ca}-heat to heating up air for dryer (kJ/h); W_p-mass of dry product in dryer (kg); $X_{w,o}$-moisture in product entering dryer (kg_{water} /$kg_{dry\ product}$); $X_{w,f}$ -moisture in product exiting the dryer (kg_{water} / $kg_{dry\ product}$); λ- latent heat of water evaporation (kJ/kg); C_{pa}-specific heat of air (kJ/ kg·°C); m_a-air mass flow (kg/h); ΔT-air temperature gradient at the inlet and outlet of the dryer chamber (°C).

2.2 Drying kinetics

Moisture content and drying rate

Moisture content samples taken at different periods of geothermal drying were analyzed. Moisture content on a dry basis (Xdb) of fresh and dehydrated slices was determined gravimetrically, with the dried mass obtained in a vacuum dryer at 70 °C until constant weight (AOAC, 1999). Moisture content using equation 4 was calculated where w_1 is the initial weight of the sample and w_2 is the sample weight during drying. The drying time for each applied drying condition was determined when the samples reached a dry-basis moisture content of 10%.

$$X_{db} = \left(\frac{W_1 - W_2}{W_1}\right) \quad (4)$$

The drying rate kinetics were calculated using the first derivative of the regression equation of moisture content versus time for each dehydration treatment studied.

Effective diffusivity

To model water transfer within the food matrix, Fick's second law for a semi-infinite flat plate was used (equation 5).

$$\frac{\partial C}{\partial t} = D \bullet \frac{\partial^2 C}{\partial X^2} \quad (5)$$

Crank's solution was used to model mass transfer. One-dimensional diffusion, moisture distribution is uniform, external resistance is negligible, and diffusivity is constantly considered. The mass transfer was determined through the estimation of the water diffusion coefficient for an infinite slab (equations 6-9).

Initial condition

$$t = 0 \quad X = X_0 \quad -L < z < L \tag{6}$$

Boundary condition

$$t > 0 \quad \frac{\partial X}{dz} = 0 \quad z = 0 \tag{7}$$

$$t > 0 \quad X = X_e \quad z = \pm L \tag{8}$$

$$\frac{X_t - X_\infty}{X_i - X_\infty} = \frac{8}{\pi^2} \sum_{n=0}^{\infty} \frac{1}{(2n+1)^2} \exp\left[-D_{eff}(2n+1)^2 \frac{\pi^2}{4L^2} t\right] \tag{9}$$

Where: D_{eff} - effective diffusivity (m^2/s); L-half thickness of the slab (m); t-drying time (s); X- moisture content of drying samples ($g_{water}/g_{dry\ matter}$). MR is the moisture ratio defined as Equation 10:

$$MR = \frac{X_t - X_\infty}{X_i - X_\infty} \tag{10}$$

In the solution of equation 2.9, the first term in the series was used due to the long drying time; all other terms of the series are negligible given the first and hence are zero.

Activation energy

The Arrhenius equation was applied to evaluate the relationship between the effective diffusivity and the geothermal drying temperature. In all cases, the activation energy was determined (equation 11).

$$D_{eff} = D_0 \exp\left(-\frac{E_a}{R \bullet T_{abs}}\right) \tag{11}$$

Where: D_0-Arrhenius constant or the constant equivalent to the diffusivity at infinitely high temperature (m^2/s), R-universal gas constant (8.314×10^{-3} kJ/mol·K), T_{abs}–absolute temperature (K), E_a-activation energy (kJ/mol).

2.3 Study of the changes in food properties during the geothermal drying process

Color

Color is one of the organoleptic properties that determines the quality of dehydrated products, with a direct effect on consumers. The effect of geothermal drying operating parameters on the color of fruit samples was monitored throughout the process (Alibas & Yilmaz, 2022; Veleşcu et al., 2023). The chromatic indices (of the L*, a*, b* system) were determined with the digital colorimeter (Model WR-10QC, 8 mm, CIELAB). The measurement was performed on fruit slices, using samples with a diameter of 3±0.05 cm to cover the entire area of the colorimeter lens. The collected spectral data were used to calculate the CIELAB'76 color parameters: L* (Luminance), a* (red-green coordinate), and b* (yellow-blue coordinate). In the study, the parameters: total color difference (ΔE), color index (Chroma), Hue angle (h°), and Browning index (BI) were determined (equations 12-16).

The color difference (ΔE) is the most important parameter of color variation because it helps to establish the differences in the L*, a*, b* system of the color changes that the sample undergoes during the drying process. The total color difference (ΔE) of the fruits before and after the drying process was calculated using equation 2.12:

$$\Delta E_{L^*a^*b^*} = \sqrt{(L^* - L_0^*)^2 + (a^* - a_0^*)^2 + (b^* - b_0^*)^2} \tag{12}$$

Where: L^*_0, a^*_0 y b^*_0 -Initial spectral parameters of the fresh sample; L^*, a^*, b^*-Final spectral parameters of the dry sample.

The color index (Chroma) is the factor that differentiates a pure tone from a gray tone. The changes in this parameter can range from 0 (matte) to 60 (intense) (equation 13):

$$Chroma = \sqrt{a^{*2} + b^{*2}} \tag{13}$$

Hue angle (h°) is defined as the degree to which a stimulus can be described as red, green, blue, and yellow. Hue angle is defined as follows:

$$when\ a^* > 0\ y\ b^* \geq 0 \rightarrow h^0_{L^*a^*b^*} = tg^{-1}\left(\frac{b^*}{a^*}\right) \tag{14}$$

$$when\ a^* < 0 \rightarrow h^0_{L^*a^*b^*} = 180 + tg^{-1}\left(\frac{b^*}{a^*}\right) \tag{15}$$

Where: the values of a* and b* are calculated and expressed in degrees: 0-red, 90-yellow, 180-green, 270-blue. The browning index (BI) is used to assess the purity of the brown color resulting from enzymatic activity and oxidation in fruits such as apples. Equation 16 was used for the calculation.

$$BI = \frac{100}{0.17}\left(\frac{a^* + 1.75 \times L^*}{5.645 \times L^* + a^* - 3.012 \times b^*} - 0.31\right) \tag{16}$$

Brix measurement during geothermal drying

Samples were removed at different periods of the geothermal drying. Brix determination was performed by refractometry (°Brix) on previously homogenized samples. After homogenization, a small apple sample was taken with a transfer pipette, and a drop of the extract was placed on the refractometer.

2.4 Experimental design and statistical analysis

A completely randomized block design experiment was used with three replicates, and an analysis of variance was conducted on the moisture content. The data analysis for this experiment was carried out using the NCSS statistical software, version 2020. ANOVA was used to determine statistically significant differences ($P \leq 0.05$).

3. Results and discussion

3.1 Drying efficiency

Temperature, airflow velocity, and relative humidity surrounding the food are key factors in removing moisture during drying. Drying efficiency depends on both the operating parameters applied and the energy consumption of the drying system. Hence, an efficient drying process requires balancing temperature, air velocity, and humidity to achieve an adequate drying time and the desired moisture removal level without compromising the dried product's final quality. Humidity plays a crucial role in drying efficiency. On the one hand, the relative humidity of the air surrounding the food directly affects the rate at which water evaporates from the product. High relative humidity in the drying chamber can reduce drying efficiency by slowing the process, while low humidity levels can speed it up. The drying efficiency as a function of energy consumed in drying apple and mango slices at different air temperatures and flow rates is presented in Table 3.

Drying efficiency was highest with the 65 °C-3.0 m/s variant, followed by the 60 °C-2.5 m/s variant for both fruits studied. Drying efficiency decreased with increasing temperature to 70°C and airflow velocity to 3.3 m/s. Similar results were reported by other authors (Beigi, 2016; Djaeni et al., 2019). During convective drying, heat and mass transfer occur simultaneously, with moisture diffusion occurring from the interior of the product to the air-food interface, followed by evaporation of water from the interface into the air stream (Tulek, 2011). Drying efficiency is highly dependent on temperature, air humidity, air velocity, and the inherent properties of the food being dried (Grau et al., 2014). High air temperatures accelerate the drying process; however, they can negatively affect the rate of moisture evaporation in the food and, consequently, the efficiency of the process. High temperatures cause hardening of the food shell because the outer surface of a material dries much faster than the core, resulting in a dry, hard, impermeable crust that prevents moisture from the core from reaching the surface of the food matrix to evaporate (Gulati & Datta, 2015).

3.2 Drying kinetics

Moisture content and drying rate

Understanding the kinetics of the drying process is essential to achieving an optimal and efficient geothermal drying process. Kinetics refers to the monitoring of the rate of water loss over processing time under the technology's specific operating conditions. The drying kinetics of dehydrated apples and mangos are shown in Figure 3. The trends in moisture kinetics were similar; in all cases, moisture content decreased exponentially with time.

In all drying curves, the moisture content decreased significantly during the first 210 min of drying, followed by a small loss of water until reaching a moisture content below 10%, at which point drying was stopped. The drying times for the experimental conditions evaluated using geothermal energy were as follows: 330, 300, and 360 min for apple slices dried at the conditions of 60 °C-2.5 m/s, 65 °C-3.0 m/s, and 70 °C-3.3 m/s, respectively; while during mango drying times of 400, 360 and 420 min were found for 60 °C-2.5 m/s, 65 °C-3.0 m/s, and 70 °C-3.3 m/s, respectively. The drying times found with the geothermal dehydrator are similar to those reported by other authors using conventional (electric) convective dryers (Paunovic et al., 2010; Cruz et al., 2015; Veleşcu

Table 3. Drying efficiency.

Products	Mean temperature (°C)	Mean airflow velocity (m/s)	Drying time (min)	Drying efficiency (%)
Apple	60	2.5	330	18±2.17
Apple	65	3.0	300	27±2.32
Apple	70	3.3	360	22±3.61
Mango	60	2.5	400	16±2.53
Mango	65	3.0	360	24±2.95
Mango	70	3.3	420	21±2.87

et al., 2023). Drying temperature and air speed significantly influenced moisture loss in the samples (P≤0.05). The temperature-airflow velocity condition of 65 °C-3.0 m/s led to lower moisture contents in the samples and shorter drying times (Figure 3), which is consistent with the experimental variant where the drying efficiency values were higher (Table 3) (P≤0.05).

At a drying temperature of 70 °C and an airflow velocity of 3.3 m/s, a reduction in moisture loss in the food was observed. It is well known that increasing temperature leads to increased evaporation and therefore to increased moisture loss. Moisture loss from the material during the drying process is limited internally and externally, with free water removed from the material (Schrader & Litchfield, 1992; Agbisit et al., 2007; Gulati & Datta, 2015). Therefore, higher temperature and drying air velocity lead to faster drying due to reduced external heat and mass transfer resistances. However, some authors (Rahman et al., 2005; Gulati & Datta, 2015) have reported that during convective drying of food matrices at temperatures of 40-60 °C, the moisture distribution is uniform since the moisture content near the surface and in the interior are very similar, i.e., drying is uniform. On the contrary, high temperatures and high air velocities induce large differences in moisture content between the surface and the core, so that the humidity drops sharply near the surface and leads to the formation of the dry outer layer that creates a barrier to moisture transport from the interior (Gulati & Datta, 2015).

The drying rate curves as a function of moisture content are shown in Figure 4. In all curves, the period of decreasing rate predominated, and in no case was the period of constant rate observed. This indicates that the drying rate decreased continuously as moisture content in the food decreased and that the diffusion mechanism controlled moisture migration within the food matrix. This drying period depends on the material properties (internal conditions), which is typical of the drying kinetics of biological materials. Similar results were reported by other authors in studies of convective drying of fruits (Toğrul, 2005; Sacilik & Elicin, 2006; Seiiedlou et al., 2010). The drying rate increased with increasing temperature and air flow rate. The difference between the drying rate curves for the experimental variants applied was highest during the first hours of the process, when humidity was higher. However, at the end of drying, where the sample had low moisture content, this difference was insignificant. Increasing the temperature of the drying air increases the rate of heat transfer between the hot airflow and the food, especially in the early stages of the drying process, when the moisture content is higher. The effect of temperature was significant in the range of 60-65°C; from 70°C onwards, a slowdown in the drying process was observed, most likely due to a superficial hardening of the food crust, which affects the rate of moisture evaporation as it prevents the moisture in the core from reaching the surface of the food and being able to evaporate.

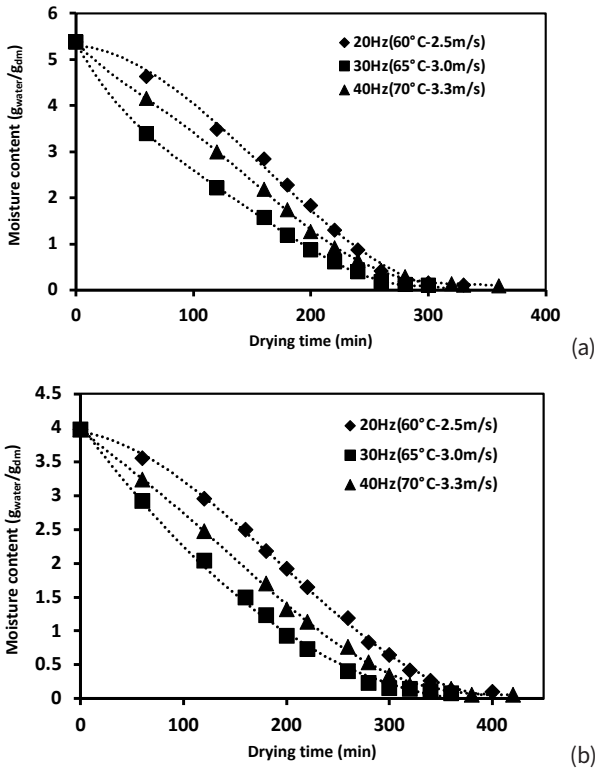

Figure 3. Moisture content observed in fruit samples during geothermal drying: a) apple; b) mango.

Modeling mass transfer

Modeling mass transfer during the geothermal fruit dehydration process is essential to ensure high-quality dried products and more energy-efficient, lower-impact processes. In this research work, Crank's solution to Fick's Law was used to calculate the effective diffusivity coefficient (D_{eff}), which describes how quickly water diffuses through a product. The moisture content data as a function of drying time were converted to a dimensionless moisture ratio (MR) and fitted to the Fick model (Figure 5). As shown in Figure 5, increasing the drying temperature and airflow velocity can significantly accelerate moisture transfer, thereby decreasing the geothermal drying time and improving process efficiency. Across all conditions analyzed, the greatest moisture loss occurred during the

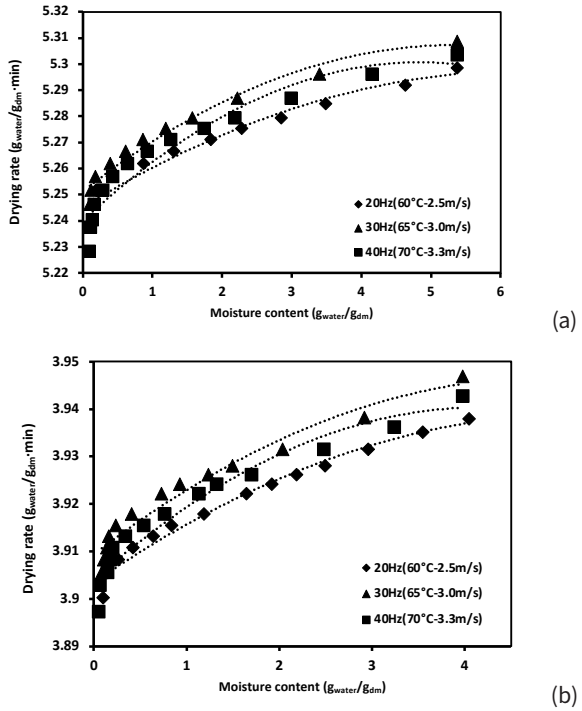

Figure 4. Drying rate based on moisture content during geothermal drying.

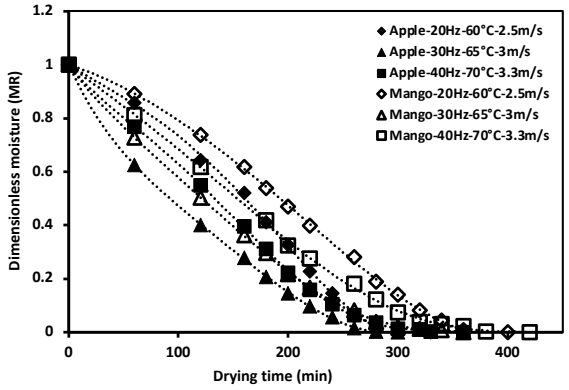

Figure 5. Dimensionless evolution of moisture content (MR) during the geothermal drying process of apple and mango samples under different temperature conditions (60, 65, 70 °C) and air flow velocity (2.5, 3.0, 3.3 m/s). Each curve represents three replicates.

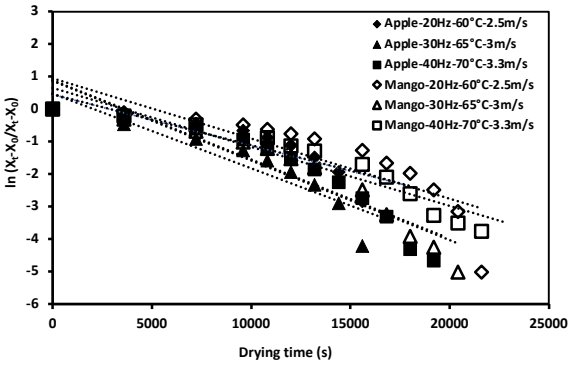

Figure 6. Moisture content versus drying time for estimating the effective moisture diffusivity.

first 200 minutes of drying, after which water loss was lower. The temperature-airflow velocity variant 65 °C-3.0 m/s promoted the greatest moisture loss in the food and a significant reduction in drying time compared to the variant 70 °C-3.3 m/s for both fruits studied (P≤ 0.05). It is well known that increasing the drying temperature can accelerate the migration of moisture from the interior of the food matrix to the surface, resulting in rapid moisture evaporation. However, very high temperatures and air velocities can slow the decrease in moisture content by forming a dry outer layer that acts as a barrier to the diffusion of moisture from the interior to the surface of the food.

Figure 6 presents the Ln (MR) graphs versus time (s) for the drying temperature-air flow velocity variants studied. The plotted curves show that increasing temperature and airflow velocity increases the slope of the straight line, which means that the effective moisture diffusivity increases. The effective diffusivity coefficient helps us understand moisture content diffusion within the food during geothermal-energy-driven drying. The effective diffusivity coefficient (Table 3.2) was obtained by determining the slope of the straight line fitted to the natural logarithm of the moisture content rate versus drying time (Figure 6). The values of *Deff* found for the experimental variants explored are within the range of those reported in the literature (Aghbashlo & Samimi-Akhijahani, 2008; Chokngamvong & Suvanjumrat, 2023; Barforoosh et al., 2014; Zeng et al., 2024). The maximum value of moisture diffusivity was $8.59 \cdot 10^{-9}\ m^2/s$ and $8.92 \cdot 10^{-9}\ m^2/s$ for the apple and mango samples, respectively, when the air velocity is 3.0 m/s and the drying temperature is 65 °C (Table 3.2). The increase in drying temperature and airflow speed caused an increase in the effective diffusivity coefficient. The increase in drying temperature can raise internal pressure and enhance the activity of water molecules within the food matrix, thereby increasing moisture diffusion and improving the drying rate. Similar results were reported by other authors (Susanti et al., 2021; Zeng et al., 2024).

Table 4. Effective diffusivity coefficient calculated with the Crank model.

Product	Mean temperature (°C)	Mean airflow velocity (m/s)	Deff·10^{-9} (m^2/s)	Determination coefficient (R^2)	Arrhenius Equation	
					Ea (kJ/mol)	R^2
Apple	60	2.5	2.43±0.22	0.92	29.18	0.94
Apple	65	3.0	8.59±0.25	0.96	27.77	0.96
Apple	70	3.3	4.38±0.18	0.95	23.44	0.93
Mango	60	2.5	4.36±0.20	0.94	26.33	0.96
Mango	65	3.0	8.92±0.19	0.97	24.54	0.96
Mango	70	3.3	5.97±0.23	0.96	21.14	0.94

The activation energy required for moisture diffusion within the food matrix is an indicator of the thermal sensitivity of effective moisture diffusivity. The values of E_a for the analyzed temperature and airflow velocity conditions are shown in Table 4. The E_a varied in the range of 23.44-29.18 kJ/mol during the geothermal drying of apples and between 21.14-26.33 kJ/mol for mango drying. The results obtained agree with the values of Ea found by other authors during fruit drying (Babalis & Belessiotis, 2004; Aghbashlo & Samimi-Akhijahani, 2008) and are within the general range for most high-moisture foods and agricultural products of 12.7 to 110 kJ/mol (Aghbashlo & Samimi-Akhijahani, 2008; Chen et al., 2023). In plant foods, surface and chemical absorption are the two forms of water present within the food matrix. In fruits such as apples and mangos with high moisture content, most of the moisture is in the form of surface absorption, so little energy is required to evaporate the water if an appropriate convective drying process is carried out. The activation energy decreases with increasing temperature and airflow velocity. The effect of drying temperature and airflow rate on Ea during drying plant foods has been verified by other authors: Waramit et al. (2021) in convective drying of cassava and Barforoosh et al. (2024) in peach drying.

Changes in food properties during the geothermal drying process

Color index

The quality of dried fruits in terms of color change has mostly been described by color differences between fresh and dried samples (Lee et al., 2003; Sacilik & Elicin, 2006; Seiidlou et al., 2010). In this study, the color change during geothermal drying of apples and mangoes was measured using color difference (Figure 7), Chroma (Figure 3.6), Hue angle (Figure 3.7), and Browning index (Figure 3.8). The color difference curves over time show that increasing drying temperature and airflow velocity led to greater color change in dried samples than in fresh fruits (Figure 3.5). In all cases, the greatest color difference was observed during the first 150 min of drying, after which the rate of color change slowed markedly. This behavior coincides with the stage of geothermal drying where moisture loss in the food is greatest (Figure 3.1). On the other hand, several authors have reported that in the first stage of drying, heat can cause degradation reactions involving the degradation of thermolabile pigments, ascorbic acid browning, and non-enzymatic Maillard browning (Ibarz et al., 1999; Maskan, 2001).

The color difference increased significantly with higher temperatures and air velocities at 70°C and 3.3 m/s (P≤ 0.05). The experimental variant temperature-airflow speed 70°C-3.3 m/s promoted the drying time, which was the longest, due to the formation of a dry, hard, and impenetrable crust on the outside of the food that limited the moisture loss during drying. Increasing the temperature to 70 °C and the long drying times increased the rate of color deterioration in the samples of the two fruits analyzed. High temperatures and long drying times can affect heat-sensitive compounds such as carbohydrates, proteins, and vitamins, causing noticeable color changes in dried fruits (Rasooli Sharabiani et al., 2021). The colour difference was remarkably higher in dried apple samples compared to dried mango samples (P≤ 0.05). The apple samples were dried without pretreatment, which justifies the greater color difference observed. The temperatures applied during geothermal drying can generate oxidation and Maillard reaction processes in the apple slices resulting in golden brown samples and a more intense scent.

Chroma* is a parameter that indicates the degree of color saturation and is proportional to color intensity (Maskan, 2001). In all cases, the chroma* value increased with increasing temperature and airflow speed (Figure

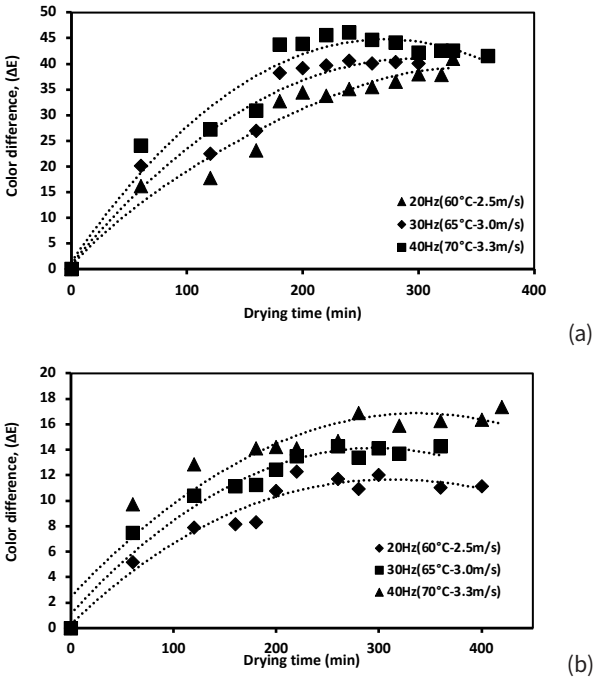

Figure 7. Total color change (ΔE) of apple (a) and mango (b) during the geothermal drying process.

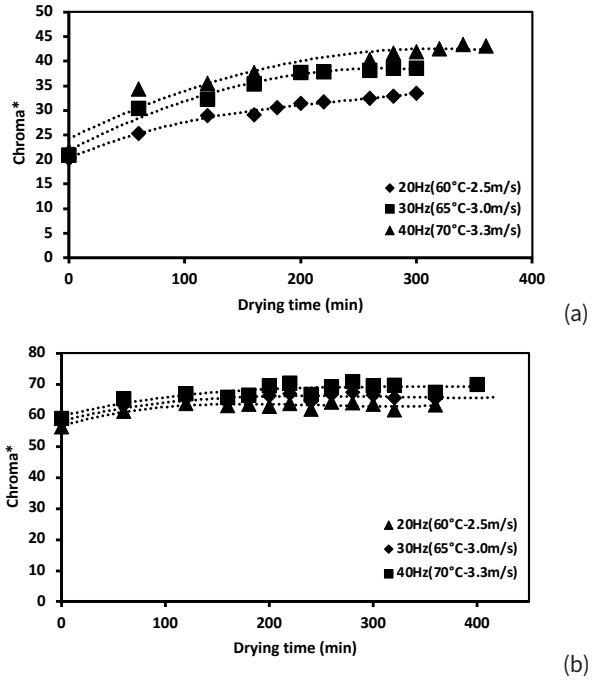

Figure 8. Chroma of apple (a) and mango (b) during the geothermal drying process.

3.6). However, the chroma* curves did not show a noticeable change with drying time, particularly during mango drying, where chroma did not change significantly over time (P≥0.05). This result corresponds to the physical observation of greater stability of the yellow color in the dried mango samples.

The Browning index (BI) indicates the purity of the brown color in samples (Figure 9). It is an important parameter in fruit drying processes, such as in apples, where enzymatic and non-enzymatic browning occurs due to temperature. In this research, the BI value varied significantly with drying time for both fruits (P≤ 0.05). Increasing drying temperature and airflow rate increased the BI value. These results suggest that the conditions of geothermal drying: temperature and airflow rate affected the quality of dried apples and mango in terms of color changes, as more brown compounds were produced in the food, more visibly observed in dried apples.

Hue angle has been widely used to characterize the color of plant foods subjected to drying processes. The Hue angle is described as follows: 0° and 360° represent the red hue, while 90°, 180°, and 270° represent the yellow, green, and blue hues, respectively (Barreiro et al., 1997; Akman et al., 2022). The hue angle values in apple samples showed an increase of 0.79-1.32, 0.76-1.37, and 0.86-1.52 for 60 °C-2.5 m/s, 65 °C-3m/s, and 70 °C-3.3m/s

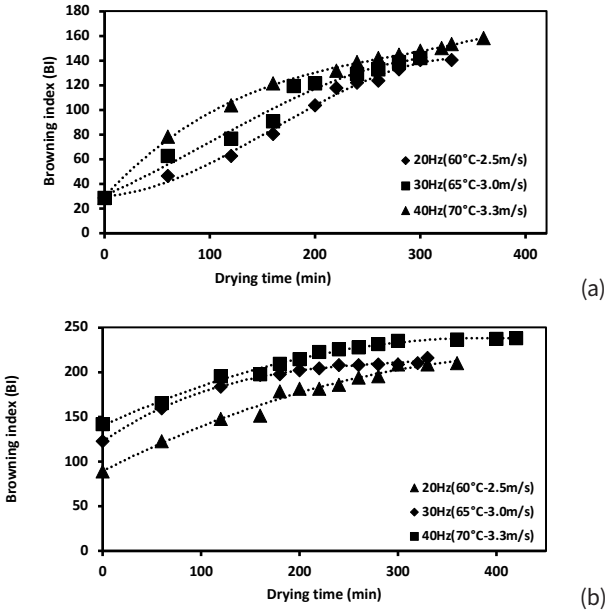

Figure 9. Browning index (BI) of apple (a) and mango (b) during the geothermal drying process.

conditions, respectively (Figure 10). A hue > 90° suggests a greener color, while a hue < 90° indicates a red-orange color. The changes in the hue angle values in mango samples were insignificant compared to the dehydrated apple samples (P≥ 0.05).

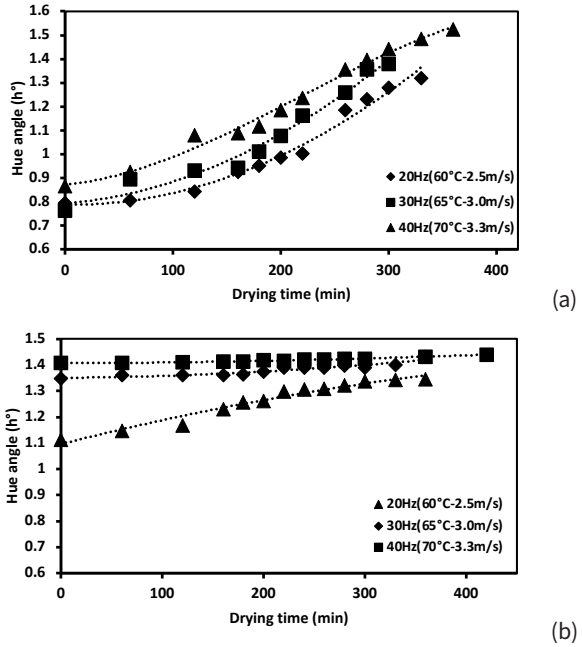

Figure 10. Hue angle of apple (a) and mango (b) during the geothermal drying process.

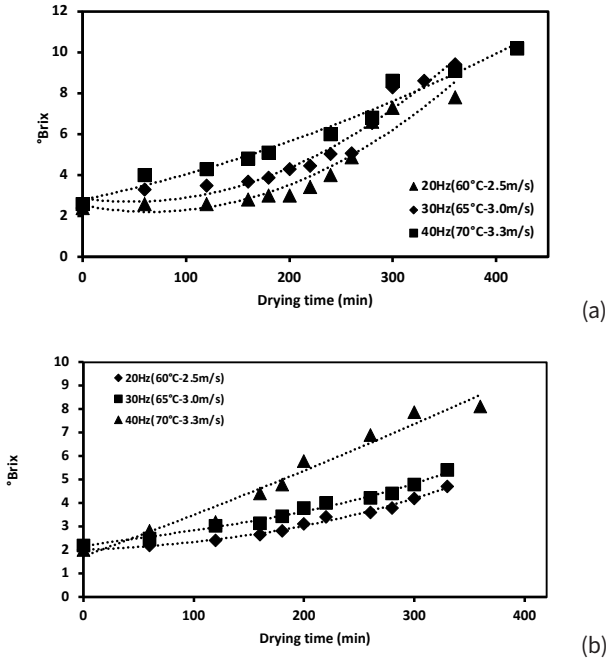

Figure 11. °Brix of apple (a) and mango (b) during geothermal drying process.

The variation of °Brix in apple and mango samples under different conditions during the geothermal drying process is shown in Figure 11. In apple samples the values varied between: 2.4-7.8, 2.4-9.4, 2.6-10.2 for the experimental conditions of 60 °C-2.5 m/s, 65 °C-3 m/s, and 70 °C-3.3 m/s, respectively; while, in mango slices the °Brix varied between 2-4.7, 2.2-5.4, 2-8.11 for the experimental conditions of 60 °C-2.5 m/s, 65 °C-3 m/s, and 70 °C-3.3 m/s, respectively. The conditions applied during geothermal drying significantly affected the increase in °Brix in the studied samples (P≤0.05). The increase in temperature and flow rate caused an increase in °Brix values in the analyzed samples. Other authors, such as Izli and Polat (2020), reported the effect of the drying process conditions on the increase in °Brix in plant foods.

Conclusions

This work demonstrated that a geothermal food dryer can achieve temperature and airflow velocity conditions sufficient to dehydrate fruit in a reasonably short time, between 5 and 7 hours, similar to that reported for conventional convective drying. To determine the benefits and disadvantages of geothermal drying, the drying kinetics were investigated. The effects of operating temperature and airflow velocity on quality properties, including moisture content, color changes, and °Brix of the dehydrated apple and mango slices, were examined. At 65°C-3.0 m/s, the greatest reduction in total drying time and higher drying efficiency were achieved, whereas at 70°C-3.3 m/s, drying slowed due to the formation of a dry surface layer that acted as a barrier to moisture removal. At 65°C-3.0 m/s, the drying rate increased and the mass transfer coefficient was higher. The color indices were strongly affected by increasing temperature and airflow velocity. The largest changes in color parameters were observed at 70°C-3.3 m/s, where darkening of the samples during drying was evident, more visible in dried apple slices than in dehydrated mango slices. °Brix values also increased with increasing temperature and air velocity. Among the applied variants, the 65°C-3.0 m/s condition was chosen as optimal, considering the results of drying kinetics, drying efficiency, process duration, and the physicochemical characteristics of the dried products (moisture content, total color difference (ΔE), color index (Chroma), Hue angle (h°), Browning index (BI), and °Brix). This study has shown that the geothermal drying process can produce high-quality dried fruits, with the added advantage of reduced processing times.

Acknowledgements

The authors wish to thank CONAHCYT for its generous support of Dr. Sahylin Muñiz-Becerá's postdoctoral fellowship.

Declaration of interest statement

The authors declare that they have no known competing financial interests or personal relationships that could have appeared to influence the work reported in this paper.

Conflict of interest

The authors does not have any type of conflict of interest to declare.

References

Agbisit, R., Alavi, S., Cheng, E., Herald, T., & Trater, A. (2007). Relationships between microstructure and mechanical properties of cellular cornstarch extrudates. *Journal of Texture Studies*, *38*(2), 199-219. https://doi.org/10.1111/j.1745-4603.2007.00094.x

Aghbashlo, M., & Samimi-Akhijahani, H. (2008). Influence of drying conditions on the effective moisture diffusivity, energy of activation and energy consumption during the thin-layer drying of berberis fruit (Berberidaceae). *Energy Conversion and Management*, *49*(10), 2865-2871. https://doi.org/10.1016/j.enconman.2008.03.009

Akman, H. E., Boyar, I., Gozlekci, S., Saracoglu, O., & Ertekin, C. (2022). Effects of convective drying of quince fruit (Cydonia oblonga) on color, antioxidant activity and phenolic compounds under various fruit juice dipping pre-treatments. *Agriculture*, *12*(8), 1224. https://doi.org/10.3390/agriculture12081224

Alibas, I., & Yilmaz, A. (2022). Microwave and convective drying kinetics and thermal properties of orange slices and effect of drying on some phytochemical parameters. *Journal of Thermal Analysis and Calorimetry*, *147*(15), 8301-8321. https://doi.org/10.1007/s10973-021-11108-3

Andritsos, N., Dalampakis, P., & Kolios, N. (2003). Use of geothermal energy for tomato drying. *GeoHeat Center Quarterly Bul*, *24*(1), 9-13. https://www.researchgate.net/profile/Paschalis-Dalampakis/publication/282134271_ANDRITSOS_N_DALAMPAKIS_P_KOLIOS_N_Use_of_geothermal_energy_for_tomato_drying_GeoHeat_Center_Quarterly_Bul_2003_241_9-13/links/56044a7708ae5e8e3f3004c7/ANDRITSOS-N-DALAMPAKIS-P-KOLIOS-N-Use-of-geothermal-energy-for-tomato-drying-GeoHeat-Center-Quarterly-Bul-2003-241-9-13.pdf

AOAC International. (1999). Official methods of analysis of AOAC International (16th ed.). AOAC International.

Babalis, S. J., & Belessiotis, V. G. (2004). Influence of the drying conditions on the drying constants and moisture diffusivity during the thin-layer drying of figs. *Journal of food Engineering*, *65*(3), 449-458. https://doi.org/10.1016/j.jfoodeng.2004.02.005

Barforoosh, M. Y., Borghaee, A. M., Rafiee, S., Minaei, S., & Beheshti, B. (2024). Determining the effective diffusivity coefficient and activation energy in thin-layer drying of Haj Kazemi peach slices and modeling drying kinetics using ANFIS. *International Journal of Low-Carbon Technologies*, *19*, 192-206. https://doi.org/10.1093/ijlct/ctad121

Barreiro, J. A., Milano, M., & Sandoval, A. J. (1997). Kinetics of colour change of double concentrated tomato paste during thermal treatment. *Journal of Food Engineering*, *33*(3-4), 359-371. https://doi.org/10.1016/s0260-8774(97)00035-6

Beigi, M. (2016). Energy efficiency and moisture diffusivity of apple slices during convective drying. *Food Science and Technology (Campinas)*, *36*(1), 145-150. https://doi.org/10.1590/1678-457x.0068

Chen, W., Hou, H., Zhang, Y., Liu, W., & Zhao, Y. (2023). Thermal and solute diffusion in α-Mg dendrite growth of Mg-5wt.% Zn alloy: A phase-field study. *Journal of Materials Research and Technology*, *24*, 8401-8413. https://doi.org/10.1016/j.jmrt.2023.05.024

Chokngamvong, S., & Suvanjumrat, C. (2023). Study of drying kinetics and activation energy for drying a pineapple piece in the crossflow dehydrator. *Case Studies in Thermal Engineering*, *49*, 103351. https://doi.org/10.1016/j.csite.2023.103351

Cruz, A. C., Guiné, R. P., & Gonçalves, J. C. (2015). Drying kinetics and product quality for convective drying of apples (cvs. Golden Delicious and Granny Smith). *International Journal of Fruit Science*, *15*(1), 54-78. https://doi.org/10.1080/15538362.2014.931166

Djaeni, M., Irfandy, F., & Utari, F. D. (2019, September). Drying rate and efficiency energy analysis of paddy drying using dehumidification with zeolite. In *Journal of Physics: Conference Series* (Vol. 1295, No. 1, p. 012049). IOP Publishing. https://doi.org/10.1088/1742-6596/1295/1/012049

Grau, R., Andres, A., & Barat, J. M. (2014). Principles of Drying. *Handbook of Fermented Meat and Poultry*, 31-38. https://doi.org/10.1002/9781118522653.ch5

Gulati, T., & Datta, A. K. (2015). Mechanistic understanding of case-hardening and texture development during drying of food materials. *Journal of Food Engineering*, *166*, 119-138. https://doi.org/10.1016/j.jfoodeng.2015.05.031

Helvacı, H. U., & Akkurt, G. G. (2014). Thermodynamic performance evaluation of a geothermal drying system. In *Progress in exergy, energy, and the environment* (pp. 331-341). Cham: Springer International Publishing. https://doi.org/10.1007/978-3-319-04681-5_29

Ibarz, A., Pagán, J., & Garza, S. (1999). Kinetic models for colour changes in pear puree during heating at relatively high temperatures. *Journal Of Food Engineering*, *39*(4), 415-422. https://doi.org/10.1016/s0260-8774(99)00032-1

Izli, N., & Polat, A. (2020). Investigation os potato drying kinetics and quality parameters applying ultrasound pre-treatments. *Latin American Applied Research - An International Journal*, *50*(4), 261-269. https://doi.org/10.52292/j.laar.2020.513

Lee, J. Y., Park, H. J., Lee, C. Y., & Choi, W. Y. (2003). Extending shelf-life of minimally processed apples with edible coatings and antibrowning agents. *LWT-Food Science and Technology*, *36*(3), 323-329. https://doi.org/10.1016/s0023-6438(03)00014-8

Li, B., Li, C., Li, T., Zeng, Z., Ou, W., & Li, C. (2019). Exergetic, Energetic, and Quality Performance Evaluation of Paddy Drying in a Novel Industrial Multi-Field Synergistic Dryer. *Energies*, *12*(23), 4588. https://doi.org/10.3390/en12234588

Maskan, M. (2001). Kinetics of colour change of kiwifruits during hot air and microwave drying. *Journal of Food Engineering*, 48(2), 169-175. https://doi.org/10.1016/s0260-8774(00)00154-0

Paunovic, D., Zlatkovic, B., & Mirkovic, D. (2010). Kinetics of drying and quality of the apple cultivars Granny Smith, Idared and Jonagold. *Journal Of Agricultural Sciences Belgrade*, *55*(3), 261-272. https://doi.org/10.2298/jas1003261p

Prasetyo, R. M., Wicaksono, A., Biddinika, M. K., & Takahashi, F. (2018). Study of geothermal direct use for coffee drying at Wayang Windu geothermal field. In *AIP Conference Proceedings* (Vol. 2026, No. 1, p. 020029). AIP Publishing LLC. https://doi.org/10.1063/1.5064989

Rahman, M. S., Al-Zakwani, I., & Guizani, N. (2005). Pore formation in apple during air-drying as a function of temperature: porosity and pore-size distribution. *Journal of The Science of Food and Agriculture*, 85(6), 979-989. https://doi.org/10.1002/jsfa.2056

Rasooli Sharabiani, V., Kaveh, M., Abdi, R., Szymanek, M., & Tanaś, W. (2021). Estimation of moisture ratio for apple drying by convective and microwave methods using artificial neural network modeling. *Scientific reports*, *11*(1), 9155. https://doi.org/10.1038/s41598-021-88270-z

Sacilik, K., & Elicin, A. K. (2006). The thin layer drying characteristics of organic apple slices. *Journal of food engineering*, *73*(3), 281-289. https://doi.org/10.1016/j.jfoodeng.2005.03.024

Schrader, G. W., & Litchfield, J. (1992). Moisture food gel during drying: measurement using magnetic resonance imaging and evaluation of the Hckian model. *Drying Technology*, *10*(2), 295-332. https://doi.org/10.1080/07373939208916440

Seiiedlou, S., Ghasemzadeh, H.R., Hamdami, N., Talati, F., & Moghaddam, M. (2010). Convective drying of apple: mathematical modeling and determination of some quality parameters. *International Journal of Agriculture and Biology, 12*, 171-178. https://www.researchgate.net/profile/Nasser-Hamdami/publication/265070331_Convective_Drying_of_Apple_Mathematical_Modeling_and_Determination_of_some_Quality_Parameters/links/54bd303b0cf27c8f2814b1ba/Convective-Drying-of-Apple-Mathematical-Modeling-and-Determination-of-some-Quality-Parameters.pdf

Sircar, A., Yadav, K., & Bist, N. (2021). Application of Geothermal Water for Food and Crop Drying. *Int. J. Innov. Res. Technol*, *8*, 2349-6002. https://www.researchgate.net/publication/352796146_Application_of_Geothermal_Water_forFood_and_Crop_Drying

Susanti, D. Y., Sediawan, W. B., Fahrurrozi, M., & Hidayat, M. (2021). Foam-mat drying in the encapsulation of red sorghum extract: Effects of xanthan gum addition on foam properties and drying kinetics. *Journal of the Saudi society of Agricultural Sciences*, *20*(4), 270-279. https://doi.org/10.1016/j.jssas.2021.02.007

Toğrul, H. (2005). Simple modeling of infrared drying of fresh apple slices. *Journal of Food Engineering*, 71(3), 311-323. https://doi.org/10.1016/j.jfoodeng.2005.03.031

Tulek, Y. (2011). Drying kinetics of oyster mushroom (Pleurotus ostreatus) in a convective hot air dryer.
https://www.sid.ir/paper/63089/en

Veleşcu, I. D., Raţu, R. N., Arsenoaia, V., Roşca, R., Cârlescu, P. M., & Ţenu, I. (2023). Research on the Process of Convective Drying of Apples and Apricots Using an Original Drying Installation. *Agriculture*, 13(4), 820.
https://doi.org/10.3390/agriculture13040820

Waramit, P., Krittakom, B., & Luampon, R. (2021). Experimental Investigation to Evaluate the Effective Moisture Diffusivity and Activation Energy of Cassava (Manihot Esculenta) under Convective Drying. *Applied Science and Engineering Progress*.
https://doi.org/10.14416/j.asep.2021.10.008

Yahya, M., Rachman, A., & Hasibuan, R. (2022). Performance analysis of solar-biomass hybrid heat pump batch-type horizontal fluidized bed dryer using multi-stage heat exchanger for paddy drying. *Energy*, *254*, 124294.
https://doi.org/10.1016/j.energy.2022.124294

Yazdani-Barforoosh, M., Mohammad Borghaee, A., Rafiee, S., Minaei, S., Beheshti, B. (2023). Determining the effective diffusivity coefficient and activation energy in thin-layer drying of Haj Kazemi peach slices and modeling drying kinetics using ANFIS. *International Journal of Low-Carbon Technologies*, 19, 192–206,
https://doi.org/10.1093/ijlct/ctad121

Zeng, Z., Han, C., Wang, Q., Yuan, H., Zhang, X., & Li, B. (2024). Analysis of drying characteristic, effective moisture diffusivity and energy, exergy and environment performance indicators during thin layer drying of tea in a convective-hot air dryer. *Frontiers in Sustainable Food Systems*, 8.
https://doi.org/10.3389/fsufs.2024.1371696